ISSN 1027-5495. Functional Materials, 33, No.1 (2026), p. 33-40
doi:http://dx.doi.org/10.15407/fm33.01.33

Explorations of the impact of strontium substitution on selected physical characteristics of the $HgBa_{1.6-x}Sr_xLa_{0.4}Ca_2Cu_3O_{8+\delta}$ superconductor

Taghreed Baqer Alwan[1], Zainab J. Neamah [2], Laheeb A. Mohammed[2], Mudatheer M. Al-Slivani [3*], Kareem A. Jasim[2]

[1] Department of Chemistry, College of Education for Pure Sciences, Ibn Al-Haitham, University of Baghdad, Iraq
[2] University of Baghdad, Department of Physics, College of Education for Pure Science, Ibn Al-Haitham
[3] Al-Furqan University, College of Education for Pure Sciences, Department of Physics, Mosul, Iraq
**mudatheeralslivani@gmail.com*

Received September 12, 2025 approved January 7, 2026

The study examines how partial substitution of strontium (Sr) for barium (Ba) in $HgBa_{1.6-x}Sr_xLa_{0.4}Ca_2Cu_3O_{8+\delta}$ superconductors influences their structural and electrical properties. Samples with Sr concentrations of x = 0, 0.1, and 0.2 were synthesized using the solid-state reaction method. X-ray diffraction (XRD) analysis confirmed that all samples maintained the tetragonal phase characteristic of the Hg-1223 structure. As Sr content increased, there were notable changes in lattice parameters and mass density. These changes were attributed to the smaller ionic radius of Sr compared to Ba, leading to a reduction in the c/a ratio. This structural modification positively influenced the superconducting properties, as indicated by the critical temperature (Tc) measurements obtained using the four-point probe method. The Tc onset increased from 127 K to 139 K, while the Tc offset rose from 118 K to 126 K as Sr content increased from 0 to 0.2. Microscopic analysis through scanning electron microscopy (SEM) revealed a reduction in grain size as the Sr concentration increased. This reduction in grain size likely minimized insulating grain boundaries, potentially enhancing the superconducting behavior. Overall, the findings suggest that Sr substitution improves superconducting properties by altering the material's microstructure and enhancing phase stability.

Keywords: Electrical Resistivity, Critical Temperature, X-Ray Diffraction, Tetragonal Structure And Superconductors.

Дослідження впливу заміщення стронцієм на вибрані фізичні характеристики надпровідника $HgBa_{1.6-x}Sr_xLa_{0.4}Ca_2Cu_3O_{8+\delta}$. *Taghreed Baqer Alwan, Zainab J. Neamah, Laheeb A. Mohammed, Mudatheer M. Al-Slivani, Kareem A. Jasim*

У дослідженні розглядається, як часткове заміщення стронцію (Sr) барієм (Ba) у надпровідниках $HgBa_{1.6-x}Sr_xLa_{0.4}Ca_2Cu_3O_{8+\delta}$ впливає на їхні структурні та електричні властивості. Зразки з концентраціями Sr x = 0, 0.1 та 0.2 були синтезовані методом твердофазної реакції. Рентгенівський дифракційний (XRD) аналіз підтвердив, що всі зразки зберігають тетрагональну фазову характеристику структури Hg-1223. Зі збільшенням вмісту Sr спостерігалися помітні зміни параметрів решітки та масової густини. Ці зміни

пояснюються меншим іонним радіусом Sr порівняно з Ba, що призводить до зменшення співвідношення c/a. Ця структурна модифікація позитивно вплинула на надпровідні властивості, що підтверджується вимірюваннями критичної температури (Tc), отриманими за допомогою методу чотириточкового зонда. Початок Tc збільшився зі 127 K до 139 K, тоді як зсув Tc збільшився зі 118 K до 126 K зі збільшенням вмісту Sr від 0 до 0,2. Мікроскопічний аналіз за допомогою скануючої електронної мікроскопії (SEM) виявив зменшення розміру зерен зі збільшенням концентрації Sr. Це зменшення розміру зерен, ймовірно, мінімізує межі ізолюючого зерна, потенційно покращуючи надпровідні властивості. Загалом, отримані результати свідчать про те, що заміщення Sr покращує надпровідні властивості, змінюючи мікроструктуру матеріалу та підвищуючи фазову стабільність.

1. Introduction

Mercury-based superconductors, $HgBa_2Ca_{n-1}Cu_nO_{2n+2+\delta}$ (with n ranging from 1 to 8, where n represents the number of Cu-O layers), are well-known for possessing one of the most intriguing homogeneous series of high-temperature superconductors due to their high transition temperatures (Tc), as demonstrated by the following sequence [1,2] Tc for n=1 (Hg-1201), is 94 K, n=2 (Hg-1212, is 127 K) and n=3 (Hg-1223) is 135 K, respectively. Under high pressure, the Tc has been further increased to 150–160 K [3]. All of the super phases of $HgBa_2Ca_{n-1}Cu_nO_{2n+2+\boldsymbol{\delta}}$ crystallize with a tetragonal structure cell and perovskite layers, according to research [4]. With the exception of the fact that the Hg-O layers are less oxygen-rich, the Hg-based superconductor structure is essentially the same as that of Tl and Cu-based superconducting. This difference is important. It has a provender for a Hg number of homologous series members [5,6]. where planes of Cu-O are present, those are responsible for the superconductivity of high-temperature [7] . The oxygen atoms are weakly linked to Hg, and depending on the preparation, their occupancy are likely to the range over the wide range. "Unfortunately, phase stability still has problems, especially in the presence of humidity and CO_2. Numerous data indicate that cation substitutions can enhance phase development and characteristics of the superconductor of Hg-1223 [8]. The Hg-1223 phase formation and critical current density can be enhanced by substituting it with a high valence type of Pb, Re, or another element [9–11]. One of a material's most crucial properties is electrical resistivity, which is also the most popular way to calculate a superconductor's Tc [12–14].

This study focuses on the impact of strontium substitution on the structural and electrical properties of the $HgBa_{1.6-x}Sr_xLa_{0.4}Ca_2Cu_3O_{8+\delta}$ superconductor. It highlights how varying levels of strontium (x = 0, 0.1, 0.2) in place of barium affect the material's transition temperature (Tc) and other key characteristics.The key outcome is the enhancement of the critical temperature (Tc), where Tc onset increased from 127 K to 139 K when x = 0.2. This study points to a potential enhancement in the superconducting performance of $HgBa_{1.6-x}Sr_xLa_{0.4}Ca_2Cu_3O_{8+\delta}$ by incorporating strontium (Sr) in place of barium (Ba). Structural changes, such as a decrease in the c/a ratio and mass density, were observed, likely due to the difference in atomic sizes between Ba and Sr. These changes are what make the material have improved superconducting properties. These results are of particular significance in the development of high-temperature superconductors, e.g. Hg-1223. Replacement of Sr can optimize the properties of the material and make it more efficient and applicable in the areas of energy storage and technological advancements. The research offers very useful information on how the behavior of superconducting materials can be finedtuned by such substitutions and this suggests that such substitutions can find use in real-life applications in energy systems and even more.

2. Experimental

A sensitive balance was used to weigh pure powders in a solid state under the materials HgO, BaO, LaO, CaO, CuO, and SrO, according to the corresponding General chemical:

$$HgO + (1.6\text{-}x)\ BaO + x\ SrO + 0.4La + 2CaO + 3CuO \rightarrow HgBa_{1.6-x}Sr_xLa_{0.4}Ca_2Cu_3O_{8+\delta}$$

The chemical formula synthesized specimens of $HgBa_{1.6-x}Sr_xLa_{0.4}Ca_2Cu_3O_{8+\delta}$ with x = 0, 0.1, and 0.2. Each reactant was weighed separately, and the powders were mixed in an agate mortar to form a homogeneous mixture, which was mixed for 30 to 50 minutes. The powder was compacted into disc-shaped pellets with a the15 mm diameter and a 2.5 mm thickness using the hydraulic press at 7 Psi for one minute. The pellets were heated to 860 °C in a Carbonite electric furnace for 60 hours before being cooled to room temperature at a heating rate of

five degrees Celsius per minute. An X-ray diffractometer of the following design (Shimadzu) was used to determine the crystal structures of the samples, with the following features: Cu K 1.5405 wavelength as a source 10-80 degrees, 8 degrees per minute scan speed, 30.0 mA current, and 40.0 kV voltage. a, b, and c lattice parameters were calculated by a computer program. Based on the Full Prof Suite toolbar [14–16], this software. The following formula has been used to estimate a volume fraction of phase from the XRD peaks of the High-1223 phase The angle and the distance between atoms was determined with the help of the analysis using the HighScore Expert software. Also the same program produced the Maner coefficients and they were calculated using the following relationship provided in Equation [17]:

$$d_{hkl} = 1/\sqrt{((h^2/a^2)+(k^2/b^2)+(l^2/c^2))} \quad (1)$$

Where I_0 is the identified phase's XRD peak intensity, the peak intensities for all XRD are I_1, I_2, ... I_n.

The following equation [12] was used to compute the densities (d_m) of the ready samples.

$$dm = \frac{Wm}{NAV} \quad (2)$$

Wm stands for molecular weight in units of amu, NA for Avogadro's number in units of particles (per gram. Ml), and *V* for the volume of a single cell in units of cm^3. The most popular method for calculating a superconductor's Tc (temperature-dependent resistivity) within the range of temperatures (77-300K) is the four-point probe method. The sample was placed inside a cryostat, which was connected to a rotary pump to generate an internal pressure of 6×10^{-3} mbar, with a digital thermometer sensor positioned near the sample. The copper wires attached to a sample were fixed using a silver paste that was dried in the oven, and these wires were used as channels for current and voltage (Fig. 1). A current source D.C power supply, delivered a 20mA current to the sample, and the voltage drop was monitored. To measure voltage, a nano-voltmeter with a sensitivity of about V was employed.

The relationship could be used to determine the resistivity (ρ) [18]:

$$\rho = \frac{V}{I}\frac{A}{t} \quad (3)$$

I and V are the variables that make up the sample's current, voltage drop between the electrodes, sample area A. and thickness (t).

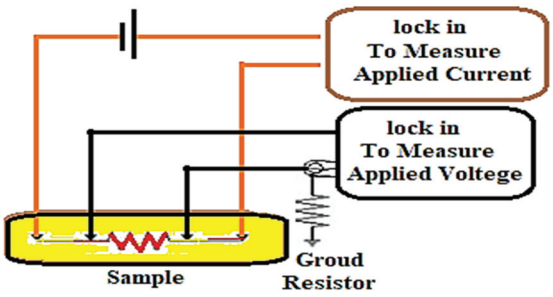

Fig. 1. resistivity (ρ) diagram measurement circuit.

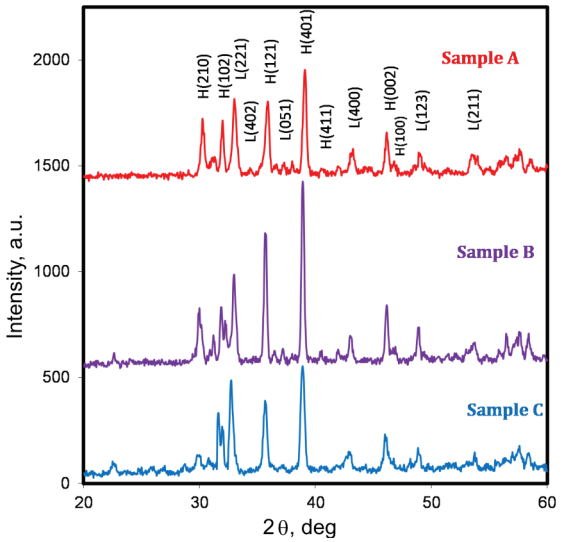

Fig. 2. Shows the X-ray diffraction patterns for the $HgBa_{1.6-x}Sr_xLa_{0.4}Ca_2Cu_3O_{8+\delta}$ samples with Sr concentrations of x = 0, 0.1, and 0.2. The patterns reveal a shift in lattice parameters, particularly in the c-axis, as the Sr content increases, demonstrating the impact of Sr substitution on the material's structural changes.

3. Results and Discussions

X-ray diffraction (XRD) patterns provide valuable insights into the structural characteristics of the samples. In this study, the XRD analysis of $HgBa_{1.6-x}Sr_xLa_{0.4}Ca_2Cu_3O_{8+\delta}$ samples with x = 0.0, 0.1, and 0.2 was performed using Bragg-Brentano geometry at room temperature. The diffraction patterns (shown in Figure 2) reveal no sharp structural peaks, confirming the amorphous nature of the samples. Figures (2a, b, and c) depict the XRD intensity patterns as a function of 2θ for the samples, showing how the substitution of Ba by Sr leads to shifts in the lattice parameters. Specifically, the ionic radii of Ba+2 (R = 1.35 Å) are larger than those of Sr+2 (R = 1.12 Å) [19,20], resulting in a shortening of the c-axis as the Ba atoms are replaced by Sr. This structural modification is reflected in the observed changes in the diffraction patterns, with a decrease in the length

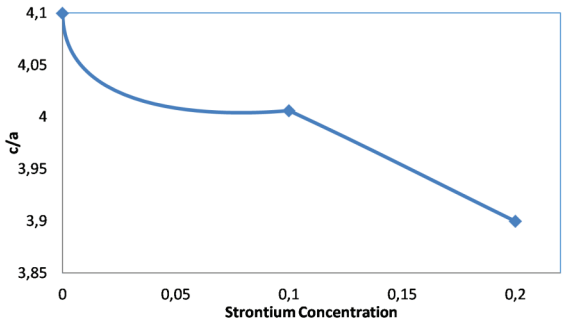

Fig. 3. Variation of the c/a parameter as a function of Sr concentration in $HgBa_{1.6-x}Sr_xLa_{0.4}Ca_2Cu_3O_{8+\delta}$ (x = 0, 0.1, and 0.2).

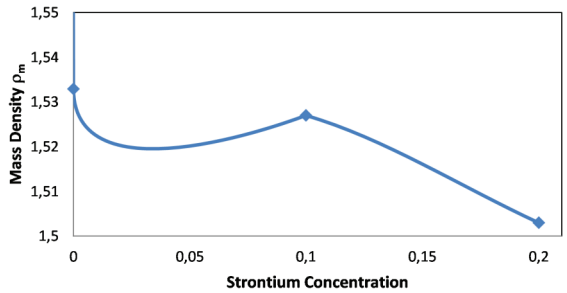

Fig. 4. Variation of mass density (ρM) as a function of Sr concentration in $HgBa_{1.6-x}Sr_xLa_{0.4}Ca_2Cu_3O_{8+\delta}$ (x = 0, 0.1, and 0.2).

of the c-axis and a shift in the diffraction peaks. The expansion of the HgO structure at the base of the diffraction peaks is indicative of the ionic size differences between Ba and Sr, impacting the overall lattice structure.

The variation of the c/a ratio with Sr concentration is illustrated in Figure 3. As seen in the figure, there is a significant drop in the c/a ratio across all three samples ($HgBa_{1.6-x}Sr_xLa_{0.4}Ca_2Cu_3O_{8+\delta}$ with x = 0, 0.1, and 0.2) as the Sr content increases. This reduction is attributed to the difference in ionic radii between Ba and Sr. Since the ionic radius of Ba (1.35 Å) is larger than that of Sr (1.12 Å), replacing Ba with Sr causes the c-axis to contract, resulting in a decrease in the c/a ratio.

Similarly, Figure 4 shows the variation of mass density (ρM) with increasing Sr concentration. A noticeable decrease in mass density is observed as the Sr content increases across the three samples. This change is due to the difference in ionic sizes between Ba and Sr, as well as the introduction of oxygen atoms into the crystal structure. The smaller ionic size of Sr reduces the number of voids in the crystal lattice, leading to a decrease in mass density [20.21].

The semi-insulating grain boundaries of High critical temperature superconductors

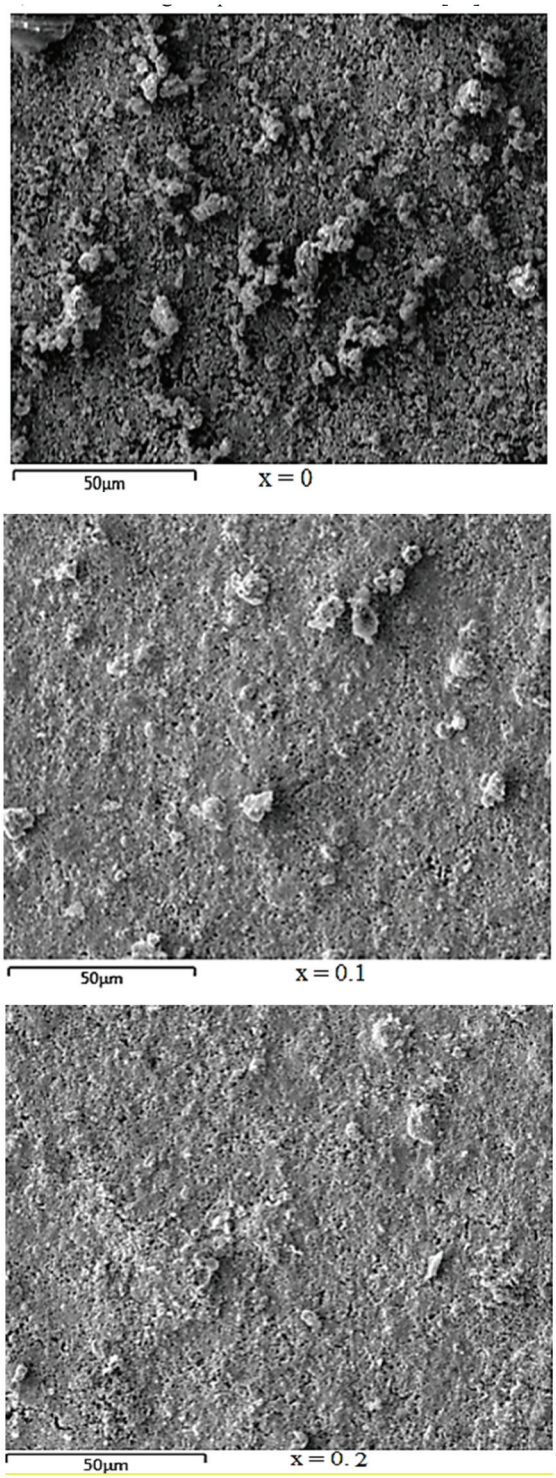

Fig. 5. SEM images showing the grain morphology of HgBa1.6-xSrxLa0.4Ca2Cu3O8+δ for x = 0 (a), 0.1 (b), and 0.2 (c), highlighting the decrease in grain size with increasing strontium concentration.

(HTSc) play a negative role in limiting the critical current and other superconducting and magnetic properties [23-31]. SEM images in Figure 5 illustrate the grain structure of sam-

Table 1 lists samples' values for lattice parameters a, b, c, C/a, mass density M, and volume fraction $V_{Ph\ (1223)}$. for various compositions of $HgBa_{1.6-x}Sr_xLa_{0.4}Ca_2Cu_3O_{8+\delta}$ (x = 0. 0.1 and 0.2)

X	Tc(OFF)(K)	Tc(ON) (K)	a(A0)	b(A0)	c(A0)	c/a	ρM (g/cm^3)	VPh-1223%
0.0	118	127	3. 77209	37721	15.41	4.0852	1.533	73.46
0.1	107	120	3.8302	3.8303	15.354	4.0015	1.527	71.48
0.2	126	139	3.8361	3.8359	15.319	3.99337	1.503	77.94

ples with varying strontium concentrations (x = 0, 0.1, and 0.2). As the concentration of strontium increases, a noticeable reduction in grain size is observed. Specifically, the average grain size decreases from 3.5 μm for x = 0 to 1.8 μm for x = 0.2, as measured using ImageJ software. This reduction in grain size is significant because it results in fewer insulating grain boundaries, which play a negative role in limiting superconductivity. By reducing these boundaries, the superconducting behavior of the material is enhanced, leading to an increased effective superconducting volume fraction. The decreased grain size allows for better connectivity between the grains, promoting a more efficient superconducting state across the material. Therefore, the critical current density and the critical temperature between and within the grains, bounded by weak bonds, are expected to increase with increasing grain size. The qualitative picture provided by the SEM images is consistent with the results obtained from various X-ray diffraction measurements, as shown in Table 1.

A scanning electron microscope (SEM) study was conducted on $HgBa_{1.6-x}Sr_xLa_{0.4}Ca_2Cu_3O_{8+\delta}$ compounds. Backscattered SEM images were taken for samples with x = 0. 0.1 and 0.2. SEM studies demonstrated that the sample with x = 0.2 was homogeneous, consisting of stone-like grains with a typical size of several microns. On the other hand, samples with x =0 and 0.1 were heterogeneous. SEM images show that stone-like and sponge-like grains coexist on the surface of the samples.

Scanning electron microscope images (Figure 5) indicate that with the addition of strontium elements to the barium site in the Hg-1223 structure, the shape changes, indicating a change in the structure of the newly formed compounds. this indicated the inter- and intra-grain changes through the susceptibility. In samples with these elements added, the grain peak decreased significantly. The grain peak overlapped with the intra-grain peak, and the intra-grain peak decreased further [32].

Using the four-probe method, electrical resistivity was assessed as an indicator of temperature by measuring the voltage and current flowing through the samples, as shown in Figure 1. Typical properties of electrical resistivity of $HgBa_{1.6-x}Sr_xLa_{0.4}Ca_2Cu_3O_{8+\delta}$ (x = 0, 0.1 and 0.2), recorded at a temperature range of 100–260 K, are shown in Figure 6. It can be seen that three samples (x = 0. 0.1 and 0.2) of the present system show quasi-linear electrical conductivity properties decreasing with decreasing temperature [2, 23].

Figure (5) shows the electrical resistance against temperature for samples of $HgLa_{0.4}Ba_{1.6-x}Sr_xCa_2Cu_3O_{8+\delta}$ $_s$trontium-free compound and containing it. It is noted from this figure that all the samples have a metallic behavior, that is, the resistivity decreases with the decrease in temperature. Likewise, there is a gradual decline in the resistivity values until they become zero at a certain value called the critical temperature Tc (onset Tc) [24,25], where the critical temperature for all samples was determined at the beginning of the resistivity drop (That is the point at which the superconductor state first emerges from the regular state.) 127, 120 and 137 K and zero resistance critical temperature $T_{c(offset)}$ at 118, 107 and 126 K. The change in the transition width was (ΔT = 19, 13 and 13). For the samples when adding strontium oxide (SrO) in the barium site of the $HgBa_{1.6-x}Sr_xLa_{0.4}Ca_2Cu_3O_{8+\delta}$ (x = 0. 0.1 and 0.2) samples, respectively, Transition temperature ($T_{c(onset)}$) changed with the strontium concentration as a result of modifications in each of a, b, c crystal lattice constants and a decrease in mass density M, which led to an increase and decrease in the volume. The highest Tc (onset) was 139 K for $HgLa_{0.4}Ba_{1.4}Sr_{0.2}La_{0.4}Ca_2Cu_3O_{8+\delta}$ when Sr=0.2, while its value in the $HgBa_{1.5-x}Sr_{0.1}La_{0.4}Ca_2Cu_3O_{8+\delta}$ compound, which is the lowest value equal to 107 K, as shown in Table 1.

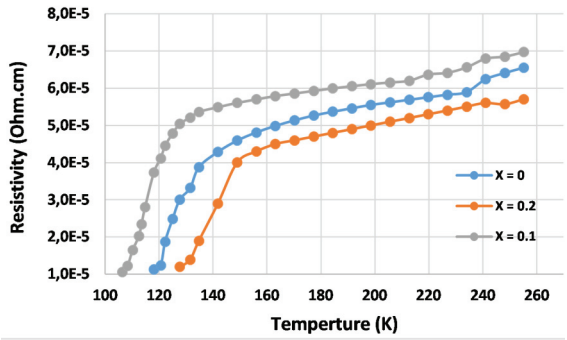

Fig. 6. Resistivity is temperature dependent for $HgBa_{1.6-x}Sr_xLa_{0.4}Ca_2Cu_3O_{8+\delta}$.

In summary, the substitution of Sr for Ba in the $HgBa_{1.6-x}Sr_xLa_{0.4}Ca_2Cu_3O_{8+\delta}$ superconductor leads to structural changes, such as a decrease in the c/a ratio and mass density, which contribute to the enhancement of the superconducting properties. Additionally, SEM analysis showed that reducing grain size improves grain connectivity, reducing insulating grain boundaries. These structural modifications, along with the significant increase in critical temperature (Tc), suggest that Sr substitution is a promising path for improving high-temperature superconductors.

Table 1 presents the values of various physical properties for different compositions of $HgBa_{1.6-x}Sr_xLa_{0.4}Ca_2Cu_3O_{8+\delta}$, where x takes values of 0.0, 0.1, and 0.2. In particular, it consists of the superconducting transition temperatures (Tc), in OFF and ON, the lattice parameters a, b and c (in A), the ratio c/a, mass density (ρ_M) in g/cm 3 and the volume fraction of the 1223 phase (VPh-1223%). This table shows the change in these parameters depending on the composition of the sample, and how the varying degrees of Sr substitution (x values) affect the structural and physical properties of the material, including the change in Tc, lattice sizes, and density. It is interesting to note that the Tc(ON) values are 120 K to 139 K, and the volume fraction of the 1223 phase belongs to 71.48% to 77.94% which means that there can be substantial changes in the superconducting properties of the material depending on its composition.

The results of my study on the superconducting properties of $HgBa_{1.6-x}Sr_xLa_{0.4}Ca_2Cu_3O_{8+\delta}$ were compared with several studies on similar modifications of Hg-1223 compounds. For example, Aljurani et al. (2021) [25] studied the influence of Tl substitution at the Hg site in $Hg_{1-x}Tl_xBa_2Ca_2Cu_3O_{8+\delta}$ and discovered that the highest critical temperature Tc was 119 K in the sample with x = 0.2, which is consistent with my results of different Tc in Sr-doped samples, with 107 K to 139 K being the highest and lowest critical temperatures, respectively. Metskhvarishvili et al. (2020) [33], studied the sol-gel and solid-state reaction approach to the synthesis of Hg-1223 compounds and reported that the approach significantly increased the transport properties and critical temperature, and although their findings indicated that the diamagnetic onset temperature of their sample was 120 K, this is comparable to effects due to Sr doping observed in my research which also indicated that the samples had similar onset temperatures. In the same way, Hermiz (2020) [34] studied the effects of Tl doping on Hg-1223 and found that the Tc in their best sample increased to 125 K, a slightly higher value than the highest Tc in my study, 139 K, indicating that Sr doping has possibly even a stronger effect on Tc than Tl. Also, the results of the research conducted by Wen et al. (2025) [35] on Hg-1223 demonstrated the exceptional Tc of the compound, 134 K, and more complicated superconducting gap structure, but the findings of my study, especially with Sr doping, provide valuable information on the need to develop and enhance Tc using doping methods and identify Sr as a dominant element in the formation of the best superconducting properties. Although these works indicate significant improvements, the comparison indicates that Sr doping provides a distinct adjustment in Hg-1223 compounds, which can outperform the work of other dopants such as Tl, Ag, and Pb, which is a better way to increase superconductivity.

4. Conclusions

The paper states that fusion of strontium (Sr) with barium (Ba) in the $HgBa_{1.6-x}Sr_xLa_{0.4}Ca_2Cu_3O_{8+\delta}$ superconductor material promotes significant innovations to the structural and electrical properties of the material. It was identified that with the increasing Sr concentration there were significant shifts in the lattice parameters, the mass density and the critical temperature Tc. In particular, Tc rose to 139 K, the transition to superconductivity occurred at an elevated temperature, and hence the behavior was more superconducting. The replacement also led to a decrease in c/a ratio and mass density that can be ascribed to smaller ionic radius size of Sr than Ba. Moreover, SEM studies showed that higher composi-

tion of Sr lowered the grain size which is beneficial to the superconductivity by minimizing the insulating grain boundaries and enhancing the amount of superconducting materials. These results demonstrate that the $HgBa_{1.6-x}Sr_xLa_{0.4}Ca_2Cu_3O_{8+\delta}$ can be doped with Sr and thus optimize its Tc properties which can be of great significances towards further development of high -Tc superconductors with enhanced stability and performance..

References

1. A. Schilling, M. Cantoni, J. D. Guo, and H. R. Ott, "Superconductivity above 130 K in the Hg–BA–Ca–Cu–O system," Nature, vol. 363, no. 6424, pp. 56-58, 1993, doi: 10.1038/363056a0.
2. A. M. Alwan, D. S. Ahmed, U. N. Saleman, and I. S. Ahmed, "Effect of the peak phase delay on an acousto-optic interaction," Journal of Al-Nahrain University Science, vol. 11, no. 3, pp. 89-97, 2008, doi: 10.22401/jnus.11.3.11.
3. P. Radaelli et al., "Structure, doping and superconductivity in $HgBa_2CaCu_2O_{6+\delta}$ (Tc ≤ 128 K)," Physica C: Superconductivity, vol. 216, no. 1-2, pp. 29-35, 1993, doi: 10.1016/0921-4534(93)90630-9.
4. K. Tokiwa et al., "Journal of Low Temperature Physics," J. Low Temp. Phys., vol. 131, no. 3/4, pp. 637-641, 2003, doi: 10.1023/a:1022992412312.
5. R. Wesche, High-temperature superconductors: Materials, properties, and applications, 1998. doi: 10.1007/978-1-4615-5075-4.
6. C. A. Passos et al., "Effects of oxygen content on the properties of the $Hg_{0.82}Re_{0.18}Ba_2Ca_2Cu_3O_{8+\delta}$ superconductor," Superconductor Science and Technology, vol. 15, no. 8, pp. 1177-1183, 2002, doi: 10.1088/0953-2048/15/8/301.
7. W. Tian, H. M. Shao, J. S. Zhu, and Y. N. Wang, "Physica Status Solidi," Physica Status Solidi (A), vol. 203, no. 11, 2006, doi: 10.1002/pssa.v203:11.
8. M. Collins, "Research: An introduction to principles, methods and practice," Evaluation and Program Planning, vol. 23, no. 4, pp. 472-473, 2000, doi: 10.1016/s0149-7189(00)00038-0.
9. A. Biju et al., "Structural and transport properties of ND doped (bi,pb)-2212," Physica C: Superconductivity, vol. 466, no. 1-2, pp. 69-75, 2007, doi: 10.1016/j.physc.2007.06.013.
10. V. Z. Kresin and S. A. Wolf, Fundamentals of superconductivity, 1990. doi: 10.1007/978-1-4899-2507-7.
11. S. H. Mahdi et al., "Preparation and study of the partial substitution of aluminum with copper on some physical properties of the compound $TlSr_2Ca_2Cu_3O_{8+\delta}$," Technologies and Materials for Renewable Energy, Environment and Sustainability: TMREES22Fr, 2023, doi: 10.1063/5.0129712.
12. J. S. Mohammed et al., "Investigate the structural properties of tl1-xhgxsr2ca2cu3o8+δ compound by using Scherrer modified equation," Technologies and Materials for Renewable Energy, Environment and Sustainability: TMREES22Fr, 2023, doi: 10.1063/5.0129140.
13. A. H. Jassim, C. A. Saleh, and K. A. Jasim, "Improving the electrical and thermal conductivity of pb1-xhgxba2ca2cu3o8+d superconducting compound by partial replacement of lead with mercury," Technologies and Materials for Renewable Energy, Environment and Sustainability: TMREES22Fr, 2023, doi: 10.1063/5.0129549.
14. R. A. Fadil, K. A. Jasim, and A. H. Shaban, "Sensitize the electrical properties of partial substitution on mercury-base superconductor manufactured by the solid reaction method," Technologies and Materials for Renewable Energy, Environment and Sustainability: TMREES21Gr, 2022, doi: 10.1063/5.0092698.
15. S. Ahmad et al., "Acoustic and thermal insulation of Nanocomposites for building material," Baghdad Science Journal, vol. 17, no. 2, p. 0494, 2020, doi: 10.21123/bsj.2020.17.2.0494.
16. K. A. Jasim, "Superconducting properties of $Hg_{0.8}Cu_{0.15}Sb_{0.05}Ba_2Ca_2Cu_3O_{8+\delta}$ ceramic with controlling sintering conditions," Journal of Superconductivity and Novel Magnetism, vol. 25, no. 6, pp. 1713-1717, 2012, doi: 10.1007/s10948-012-1507-3.
17. M. M. Al-Slivani, M. A. Hammod, and M. A. Abed, "Partial substitution effect of silver on the structural and electrical properties of high-temperature superconductor ($(Bi_{2-x}Ag_xBa_2Ca_2CO_2Cu_3O_{10+\delta})$)," Ochrona przed Korozją, vol. 1, no. 3, pp. 15–20, 2025, doi: 10.15199/40.2025.3.2.
18. M. M. Al-Slivani, M. A. Hammod, and M. A. Abed, "Double partial substitution effect of silver (Ag) and strontium (Sr) on the structural and electrical properties of high-temperature $Bi_{2-x}Ag_xBa_{2-y}Sr_yCa_2Cu_3O_{10+\delta}$ superconductor," Functional Materials, vol. 32, pp. 42–49, 2025, doi: 10.15407/fm32.01.42.
19. R. S. Al-Khafaji and K. A. Jasim, "Dependence of the microstructure specifications of earth metal lanthanum La substituted Bi2Ba2CaCu2–XLaXO8+δ on cation vacancies," AIMS Materials Science, vol. 8, no. 4, pp. 550-559, 2021, doi: 10.3934/matersci.2021034.

20. B. A. Omar, S. J. Fathi, and K. A. Jasim, "Effect of Zn on the structural and electrical properties of high-temperature $HgBa_2Ca_2Cu_3O_{8+\delta}$ superconductor," AIP Conference Proceedings, 2018, doi: 10.1063/1.5039234.
21. I. Hamadneh, Y. W. Kuan, L. T. Hui, and R. Abd-Shukor, "undefined," Materials Letters, vol. 60, no. 6, pp. 734-736, 2006, doi: 10.1016/j.matlet.2005.10.002.
22. H. M. Haider and K. A. Jasim, "Effect of composition and dielectric properties for (YBCO) superconductor compound in different preparation methods," Ibn Al-Haitham Journal For Pure and Applied Sciences, vol. 33, no. 1, p. 17, 2020, doi: 10.30526/33.1.2372.
23. H. M. Haider and K. A. Jasim, "Studying the effect of the methods of various preparation of $Bi_2Ba_2Ca_2Cu_{2.8}Zn_{0.2}O_{10+\delta}$ superconducting compound," AIP Conference Proceedings, 2019, doi: 10.1063/1.5116959.
24. L. A. Mohammed and K. A. Jasim, "Synthesis and study of the structural and electrical and mechanical properties of high-temperature superconductor Tl0.5Pb0.5Ba2Can-1CunxNiO2n+3-Îδ substituted with nickel oxide for n=3," Ibn Al-Haitham Journal for Pure and Applied Sciences, vol. 31, no. 3, pp. 26-32, 2018, doi: 10.30526/31.3.2024.
25. B. A. Aljurani, G. Hermiz, and M. Alias, "Superconductivity measurements of (Hg,Tl)-1223 compound prepared in capsule," Iraqi Journal of Science, pp. 2934-2939, 2021, doi: 10.24996/ijs.2021.62.9.9.
26. K. A. Jasim, T. J. Alwan, H. K. Al-Lamy, and H. L. Mansour, "Improvements of superconducting properties of $Hg_{0.6}Pb_{0.25}Sb_{0.15}Ba_2Ca_2Cu_3O_{8+\delta}$ ceramic by controlling the sintering time," Journal of Superconductivity and Novel Magnetism, vol. 24, no. 6, pp. 1963–1966, 2011.
27. L. A. Mohammed, K. A. Jasim, "Improvement the superconducting properties of $TlBa_2Ca_2Cu_{3x}NiO_{9-\delta}$ superconducting compound by partial substitution of copper with nickel oxide," Energy Procedia, vol. 157, pp. 135–142, 2019.
28. S. H. Mahdi, W. H. Jassim, I. A. Hamad, K. A. Jasima, "Epoxy/Silicone Rubber Blends for Voltage Insulators and Capacitors Applications," Energy Procedia, vol. 119, pp. 501–506, 2017.
29. K. A. Jasim, S. A. Makki, A. A. Almohsin, "Comparison study of transition temperature between the superconducting compounds $Tl_{0.9}Pb_{0.1}Ba_2Ca_2Cu_3O_9$, $Tl_{0.9}Sb_{0.1}Ba_2Ca_2Cu_3O_{9-\delta}$ and $Tl_{0.9}Cr_{0.1}Ba_2Ca_2Cu_3O_{9-\delta}$," Physics Procedia, vol. 55, pp. 336–341, 2014.
30. K. A. Jasim, T. J. Alwan, K. H. Mahdi, H. L. Mansour, "The effect of neutron irradiation on the properties of Tl0.6Pb0.3Cd0.1Ba2Ca2Cu3O9-δ superconductors," Turkish Journal of Physics, vol. 37, no. 2, pp. 237–241, 2013, doi: 10.3906/fiz-1203-16.
31. K. A. Jasim, W. H. Jassim, S. H. Mahdi, "The effect of sunlight on medium density polyethylene Water pipes," Energy Procedia, vol. 119, pp. 650–655, 2017, doi: 10.1016/j.egypro.2017.07.091.
32. K. A. Jasim, T. J. Alwan, K. H. Mahdi, H. L. Mansour, "The effect of neutron irradiation on the properties of $Tl_{0.6}Pb_{0.3}Cd_{0.1}Ba_2Ca_2Cu_3O_{9-\delta}$ superconductors," Turkish Journal of Physics, vol. 37, no. 2, pp. 237–241, 2013, doi: 10.3906/fiz-1203-16.
33. I. R. Metskhvarishvili, G. N. Dgebuadze, T. E. Lobzhanidze, B. G. Bendeliani, M. R. Metskhvarishvili, and M. Sh. Rusia, "SG and SSR approach in the preparation of precursors and influence on superconducting properties of Tl-1223 superconductors," *Sukhumi Institute of Physics and Technology*, 2020.
34. G. Y. Hermiz, "The Role of Tl Substitution on Superconducting Properties for Hg-1223 System," *1st International Conference in Physical Science and Advance Materials*, IOP Conf. Series: Materials Science and Engineering, vol. 757, p. 012058, 2020.
35. C. Wen, Z. Hou, A. Akbari, K. Chen, W. Hong, H. Yang, I. Eremin, Y. Li, and H. H. Wen, "Unprecedentedly large gap in $HgBa_2Ca_2Cu_3O_{8+\delta}$ with the highest Tc at ambient pressure," *npj Quantum Materials*, vol. 10, p. 20, 2025.